Aliyar Javadi, Saeid Dowlati, Sara Shourni, Sherly Rusli, Kerstin Eckert, Reinhard Miller, Matthias Kraume

Enzymatic Hydrolysis of Triglycerides at the Water–Oil Interface Studied via Interfacial Rheology Analysis of Lipase Adsorption Layers

Citation details
Javadi, A., Dowlati, S., Shourni, S., Rusli, S., Eckert, K., Miller, R., & Kraume, M. (2021). Enzymatic Hydrolysis of Triglycerides at the Water–Oil Interface Studied via Interfacial Rheology Analysis of Lipase Adsorption Layers. In Langmuir (Vol. 37, Issue 44, pp. 12919–12928). American Chemical Society (ACS). https://doi.org/10.1021/acs.langmuir.1c01963.

Enzymatic Hydrolysis of Triglycerides at Water–Oil Interface Studied via Interfacial Dilational Rheology of Lipase Adsorption Layers

Aliyar Javadi[1, 2, 3, 4, *], Saeid Dowlati[1, 2], Sara Shourni[2], Sherly Rusli[1], Kerstin Eckert[3, 4], Reinhard Miller[5] and Matthias Kraume[1]

1. *Technische Universität Berlin, Chair of Chemical and Process Engineering, Straße des 17. Juni135,10623 Berlin, Germany.*
2. *Chemical Engineering Department, College of Engineering, University of Tehran, 14395-515, Tehran, Iran.*
3. *Institute of Fluid Dynamics, Helmholtz-Zentrum Dresden-Rossendorf (HZDR), Bautzner Landstraße 400, 01328 Dresden, Germany.*
4. *Institute of Process Engineering and Environmental Technology, Technical University Dresden, D-01069 Dresden, Germany.*
5. *Technical University Darmstadt, Hochschulstraße 12, D-64289 Darmstadt, Germany.*

* Corresponding Author: Javadi.aliyar@hzdr.de, javadi.aliyar@ut.ac.ir

Abstract

The enzymatic hydrolysis of sunflower oil occurs at the water–oil interface. Therefore, the characterization of dynamic interfacial phenomena is essential for understanding the related mechanisms for process optimizations. Most of the available research works for this purpose deal with averaged interfacial properties determined via reaction kinetics and dynamic surface tension measurements. In addition to the classical approach for dynamic surface tension measurements, here, the evolution of the dilational viscoelasticity of the lipase adsorbed layer at the water–oil interface is characterized using profile analysis tensiometry. It is observed that lipase exhibits nonlinear dilational rheology depending on the concentration and age of the adsorbed layer. For reactive water–oil interfaces, the response of the interfacial tension to the sinusoidal area perturbations becomes more asymmetric with time. Surface-active products of the enzymatic hydrolysis of triglycerides render the interface less elastic during compression compared to the expansion path. The lipolysis products can facilitate desorption upon compression while inhibiting adsorption upon expansion of the interface. Lissajous plots provide an insight into how the hysteresis effect leads to different interfacial tensions along the expansion and compression routes. Also, the droplet shape increasingly deviates from a Laplacian shape, demonstrating an irreversible film formation during aging and ongoing hydrolysis reaction, which supports our findings via interfacial elasticity analysis.

Keywords

Lipase Adsorption, Dilational Rheology, Enzymatic Reactions, Reactive Interface, Interfacial Elasticity, Drop Profile Analysis Tensiometry.

Introduction

Lipase is an enzyme responsible for the hydrolysis of triglycerides [1]. Triglycerides, or triacylglycerols, are esters with a glycerol backbone bound to three fatty acid chains [2]. Naturally occurring triglycerides are from plants and animals [3]. A lipase molecule can cleave the triglyceride ester bonds, producing diglyceride, monoglyceride, glycerol, and free fatty acids [4].

Transesterification is the substitution of the functional group of an ester with the functional group of an alcohol (alcoholysis), an acid (acidolysis), or another ester (interesterification) [5]. In triglycerides, transesterification can occur for each of the three ester groups. Transesterification of triglycerides with alcohol produces fatty acid alkyl esters (FAAE) [6-8], which are the main components of *biodiesel*, a sustainable source of eco-friendly energy [9]. Biodiesel production can be catalyzed either chemically or enzymatically [10].

The source of lipases determines how they hydrolyze triglycerides [1]. Lipase from *Candida rugosa* is non-regiospecific; it shows no positional specificity and cleaves all three (Sn-1,2,3) positions in the triglyceride, where Sn stands for stereospecific numbering of carbons [11]. In contrast, gastric and pancreatic lipases are Sn-1,3 regiospecific, meaning that they only cleave the outer ester bonds in the triglycerides and Sn-2 monoglycerides remain unaffected [12]. However, a pH-dependent acyl group migration can convert Sn-2 into hydrolyzable Sn-1,3 monoglycerides [13].

Lipases are water-soluble proteins and their lipolysis occurs at the water–oil interface [1]. In bulk, lipase is enzymatically inactive [14]. A conformational change in the lipase structure upon its interfacial adsorption makes the active site available for the substrate, i.e., glycerides [15]. Lipase attaches to the interface via *van der Waals*, hydrophobic interactions, or dispersion forces [16]; however, low molecular weight surfactants can remove it from the interface [17, 18]. The reactive interfacial composition between an aqueous lipase solution and an apolar lipid phase evolves over time since the reaction products are also surface-active. The displacement of lipase from the interface leads to self-regulation of the lipolysis reaction [11, 12]. So, the assumption of mere adsorption does not sufficiently explain the interfacial behavior of lipase at water–oil interfaces.

High interfacial tension can lead to lipase denaturation, while a high interfacial pressure can give rise to the inactivation of the lipase molecules [19, 20]. Thus, other interfacial active agents have an impact on the enzymatic activity of the lipase. All reaction products of enzymatic hydrolysis of lipids have interfacial activity. The electrostatic and hydrophobic interactions between the anionic headgroups of the fatty acid carboxylates and their alkyl chains with oppositely charged sites and the hydrophobic patches of the lipase molecules significantly impact the catalytic behavior of the lipase [21]. Diglycerides partition between the oil phase and the interface, while the monoglycerides partition between both bulk phases and the interface [22]. It is shown that Sn-2 monopalmitin can remove both pancreatic lipase and tricaprylin from the

interface and decrease the rate of triglyceride hydrolysis [23]. Sn-2 monoglycerides are also more interfacial active than diglycerides and fatty acid salts and, thus, can dominate the interface given that enough time is available [22]. However, as mentioned above, lipase from Candida rugosa is a non-regiospecific lipase and, therefore, is not expelled from the interface upon enzymatic fat digestion because of transesterification of Sn-2 monoglycerides into fatty acid alkyl esters and glycerol [12]. Moreover, another interfacial feature of a lipase adsorbed layer is the formation of a skin-like film at the interface as a result of protein unfolding and covalent crosslinking. This feature emerges upon aging and compression of the lipase adsorbed layer as wrinkles [24].

Dynamic tensiometry and dilational rheology have been proposed to study the chemical reactions, such as lipase hydrolysis, in single droplets [25, 26]. Here, we have investigated the interfacial dilational rheology of lipase at reactive and nonreactive interfaces. To this aim, the viscoelastic behavior of adsorbed layers of *Candida rugosa* lipase at the water–sunflower oil (SFO) interface is studied. Some of the results are compared with the lipase viscoelasticity at the water–air and water–heptane interfaces. A *profile analysis tensiometer* (*PAT-1*) is used to conduct dynamic interfacial tension (IFT) and interfacial dilational elasticity measurements.

Materials and Methods

Chemicals

Lipomod^{TM} *34P-L034P* lipase from *Candida rugosa* was provided by *Biocatalysts Ltd* (*Cardiff, UK*) as a white powder with an activity of 115000 $U \cdot g^{-1}$. The sunflower oil (SFO) was supplied by *Oleon GmbH* (*Emmerich am Rhein, Germany*) and purified with column chromatography using *Florisil*® 100-200 mesh, based on the method addressed elsewhere [27]. n-heptane (assay GC ≥ 99.3%) was purchased from *Merck (Darmstadt, Germany)* and purified by passing through a chromatographic column. The buffer solutions were prepared using phosphate-buffered saline from *Sigma-Aldrich (Merck, Darmstadt, Germany*) with a pH of *7.4* and an ionic strength of *0.17 M* at room temperature.

The high concentration lipase solutions were prepared by adding the dry lipase powder to the phosphate-buffered saline solutions under mild stirring conditions. Then it has been diluted with buffer solution for preparing lower concentrations. The lipase solutions have been prepared fresh and used within a week, with relevant storage at 4 °C.

Profile Analysis Tensiometer (PAT-1)

The *Profile Analysis Tensiometer (PAT-1)* is an instrument manufactured by *SINTERFACE Technologies (Berlin, Germany)* for measuring surface and interfacial tensions and is schematically represented in Figure

1. PAT captures high-resolution images of a droplet of a few microliters volume formed at the tip of a capillary. The profile of the droplet is digitized using image processing techniques. The theoretical droplet profile derived from the *Young-Laplace equation* (*Eq. 1*) is then fitted to the experimental profile coordinates by adjusting the IFT, γ, as the only fitting parameter:

$$\Delta p = \gamma\left(\frac{1}{R_1} + \frac{1}{R_2}\right) \quad (1)$$

where Δp is the pressure difference across the interface, and R_1 and R_2 are the principal radii of curvature in the drop apex. The methodology has been discussed in detail elsewhere [28]. The standard deviation (STD) is a parameter that quantifies the difference between the theoretical Young–Laplace equation and experimental droplet profiles and serves as a parameter for the quality of fitting:

$$STD = \left(\frac{1}{N}\sum_{i=1}^{N}(e_i - \mu)^2\right)^{1/2} \quad (2)$$

where N is the number of points in the discretized droplet profile, e is the x-error between the theoretical and experimental droplet profiles, $e_i = x_i^{theo} - x_i^{expr}$, and μ is the mean of the x-errors.

Each PAT test was conducted at least three times to ensure the reproducibility of the data. Also, the measurements with similar conditions were cross-checked to validate the results. Before starting the measurements at each session, the PAT setup was calibrated by measuring the surface tension of water at room temperature to obtain ~72.8 mN·m^{-1} at 20 °C. An error of ±0.2 mN·m^{-1} during calibration is expected due to ambient conditions. After accurate calibration, the surface/interfacial tension measuring accuracy narrows down to the setup resolution: ±0.01 mN·m^{-1}.

Interfacial Dilational Rheology

Imposing interfacial area oscillations to a drop surface is a way to characterize the dilational viscoelasticity of the interfacial layer. To this aim, a set of harmonic perturbations is applied to the interfacial area of a pendant drop as a common practice. Then, the IFT responses to these perturbations are recorded and analyzed to determine the viscoelastic properties of the adsorbed layer. A sinusoidal perturbation of an interfacial area, $A(t)$, can be imposed as follows [29]:

$$A(t) - A_0 = \Delta A(t) = A_{amp} \cdot sin(\omega t) \quad (3)$$

where A_0 is the average interfacial area before the oscillation, and A_{amp} and ω are the amplitude and frequency of the area oscillation. A sinusoidal perturbation can be divided into two periods: expansion, during which $dA/dt > 0$, and compression, during which $dA/dt < 0$. The linear response of IFT, $\gamma(t)$, takes the form:

$$\gamma(t) - \gamma_0 = \Delta\gamma(t) = \gamma_{amp} \cdot sin(\omega t + \varphi) \quad (4)$$

where γ_0 is the equilibrium IFT before starting the oscillations, and γ_{amp} and φ are the amplitude and phase shift of the IFT response. The complex viscoelasticity, $\varepsilon(i\omega)$, is a transfer function transforming the input signal into the output signal in the frequency domain [30, 31]:

$$\varepsilon(i\omega) = \frac{\mathcal{F}[\Delta\gamma(t)]}{\mathcal{F}[ln(\Delta A(t))]} \cong A_0 \frac{\mathcal{F}[\Delta\gamma(t)]}{\mathcal{F}[\Delta A(t)]} \quad (5)$$

$$\varepsilon(i\omega) = \varepsilon'(\omega) + i \cdot \varepsilon''(\omega) = \varepsilon_d(\omega) + i \cdot \omega \cdot \eta_d(\omega) \quad (6)$$

where $\mathcal{F}$ is the Fourier transform operator, ε' is the real part of the complex interfacial viscoelasticity and equals to the dilational elasticity (ε_d), ε'' is the imaginary part, i is the imaginary unit, and η_d is the dilational viscosity. In a linear domain of the IFT response, the dilational elasticity and viscosity are functions of only the frequency (ω), making the transfer function additive and uniform [29]. In this case, t can be eliminated between Eqs. 2 and 3, resulting in:

$$A_D^2 + \gamma_D^2 - 2cos(\varphi) \cdot A_D \cdot \gamma_D = sin^2(\varphi) \quad (7)$$

where $A_D = \Delta A(t)/A_{amp}$ and $\gamma_D = \Delta\gamma(t)/\gamma_{amp}$ are the dimensionless area and IFT. Eq. 6 is an ellipse, the inclination angle and width of which are measures of the dilational elasticity and viscosity. In an inviscid interfacial layer ($\varphi = 0$), Eq. 6 becomes a line ($A_D = \gamma_D$). This ellipse is the Lissajous plot of an adsorbed layer with linear IFT response to the harmonic area perturbations. Under a nonlinear interfacial regime, the Lissajous plot shape can deform in different ways, some of which are discussed in the results section.

The linear rheology holds for steady-state and small-area perturbations. For nonequilibrium states, e.g., early-time adsorption or reactive interfaces, and nonlinear rheology, e.g., large-area perturbations, the IFT responses deviate from this linearity. There are some methods to treat the nonlinear interfacial dilational rheology, such as Volterra series, Fourier transform operation, Fourier expansion series, stress decomposition method, Lissajous plots, and polynomial series [32]. Here, we use the Fourier expansion series and Lissajous plots for the quantitative and qualitative data analysis.

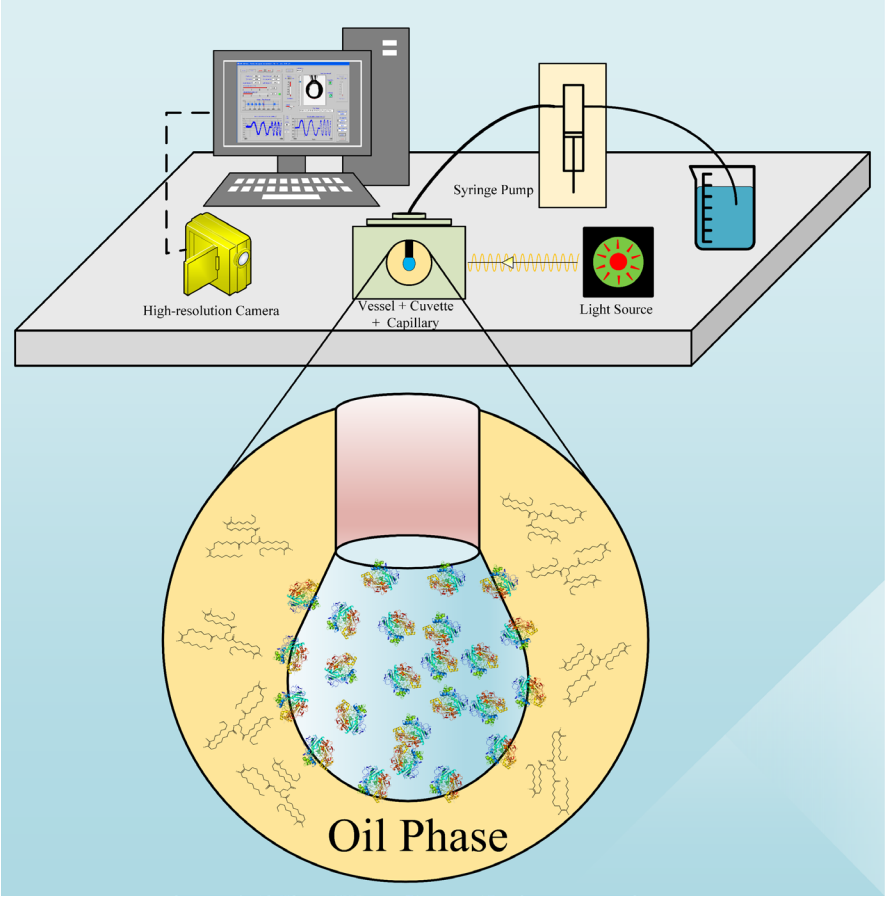

Figure 1 Schematic representations of the Profile Analysis Tensiometer (PAT) and lipase adsorbed layer at water–oil interface.

Results

Interfacial Tension between Oil and Lipase Solutions

In order to develop its catalytic activity, lipase diffuses from the aqueous droplet bulk to the interface to get in contact with the hydrophobic lipids. The dynamics of adsorption of lipase is shown in Figure 2. Note that in the absence of any lipase in the system, we observe very small IFT oscillations caused by the smallest amounts of impurities in the sunflower oil sample. Lipase adsorption significantly increases the interfacial elasticity of a water–oil interface. The removal of lipase macromolecules from the interface is energy-intensive. During interfacial oscillations, lipase as a macromolecule cannot desorb from or readsorb at the interface fast enough during subsequent compressions and expansions of the oscillation cycles to keep the interfacial concentration in thermodynamic equilibrium with the bulk concentration. Also, upon lipase adsorption, protein unfolding occurs due to the tendency of hydrophobic internal residues to become better exposed to the apolar oil phase [15, 33]. These two effects give rise to the higher elasticity of the lipase

adsorbed layers. The solution of higher lipase concentration, 2.5 mg·mL^{-1}, has a lower IFT and higher elasticity, showing that the increasing interfacial interactions between the unfolded lipase molecules at higher concentrations can resist lipase desorption and readsorption during compressions and expansions. Also, the initial IFT value for the buffer–SFO interface of about 24 mN·m^{-1} is rather low and points to the fact of small amounts of impurities [34], which, however, are not essential for the target of this study on the enzymatic reaction of lipase at the water–SFO interface via measurements of the dilational interfacial viscoelasticity.

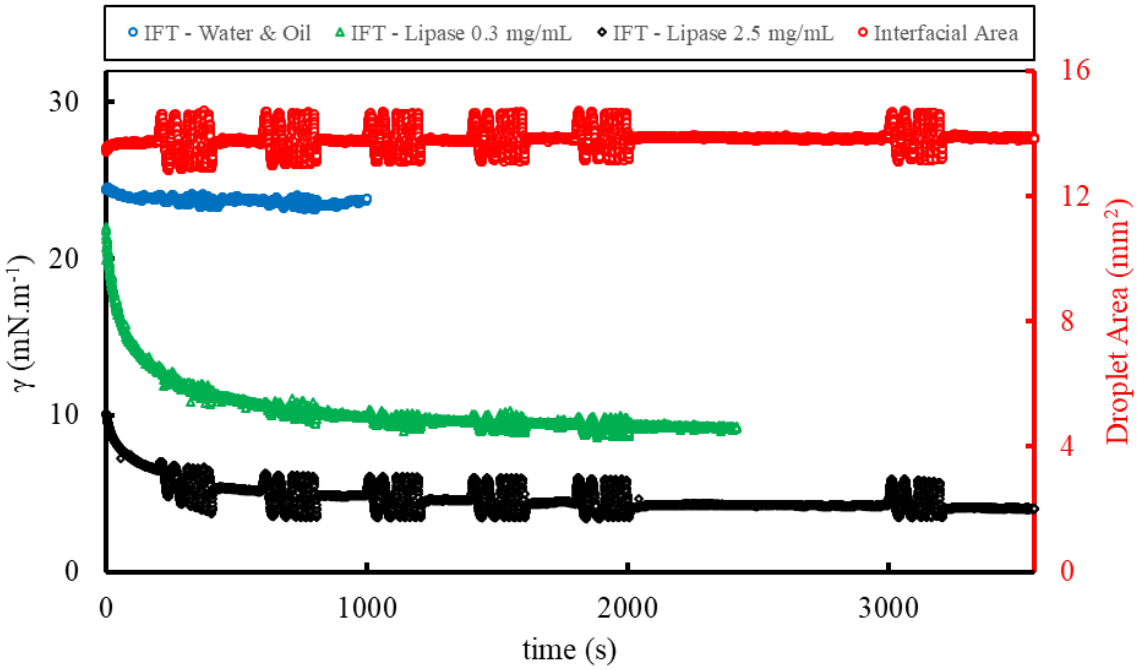

Figure 2- (○) Interfacial area with sinusoidal perturbations of 0.5 mm^3 volumetric amplitude (~1 mm^2 area amplitude) and 0.05 and 0.02 Hz frequencies for three different aqueous droplets with a volume of 5.0 mm^3 inside the sunflower oil phase and their interfacial tension response: (○) buffer droplet with no lipase, (△) 0.3 mg·mL^{-1}, and (◇) 2.5 mg·mL^{-1} lipase solution droplets.

Low Concentrations of Lipase

The IFT and STD of a *0.3 mg·mL^{-1}* lipase solution in different time intervals are shown in Figure 3. The amplitudes of the IFT response caused by the sinusoidal area perturbations increase with time due to the increasing interfacial concentration of the adsorbed lipase. Figure 3(b) shows that the IFT trend is downward, i.e., the adsorbed layer has not fully reached the equilibrium state yet. In cases like this, the non-oscillating IFT trendline in the response should be considered to make elasticity calculations more accurate using Eq. 4, i.e., the IFT values should be detrended. To this aim, it is assumed that $\Delta\gamma(t) = \gamma(t) - f(t)$, where $f(t)$ is the non-oscillating component of the IFT response [35]. Here, we have used linear $f(t)$, as

denoted by green lines.

In cases Figure 3(c–f), the increasing IFT amplitudes reflect that the elasticities increase with time. In cases (b–f), the STD values are low and uniform, meaning no severe deviation of the droplet profiles from the ideal Laplacian shape occurred during this set of experiments.

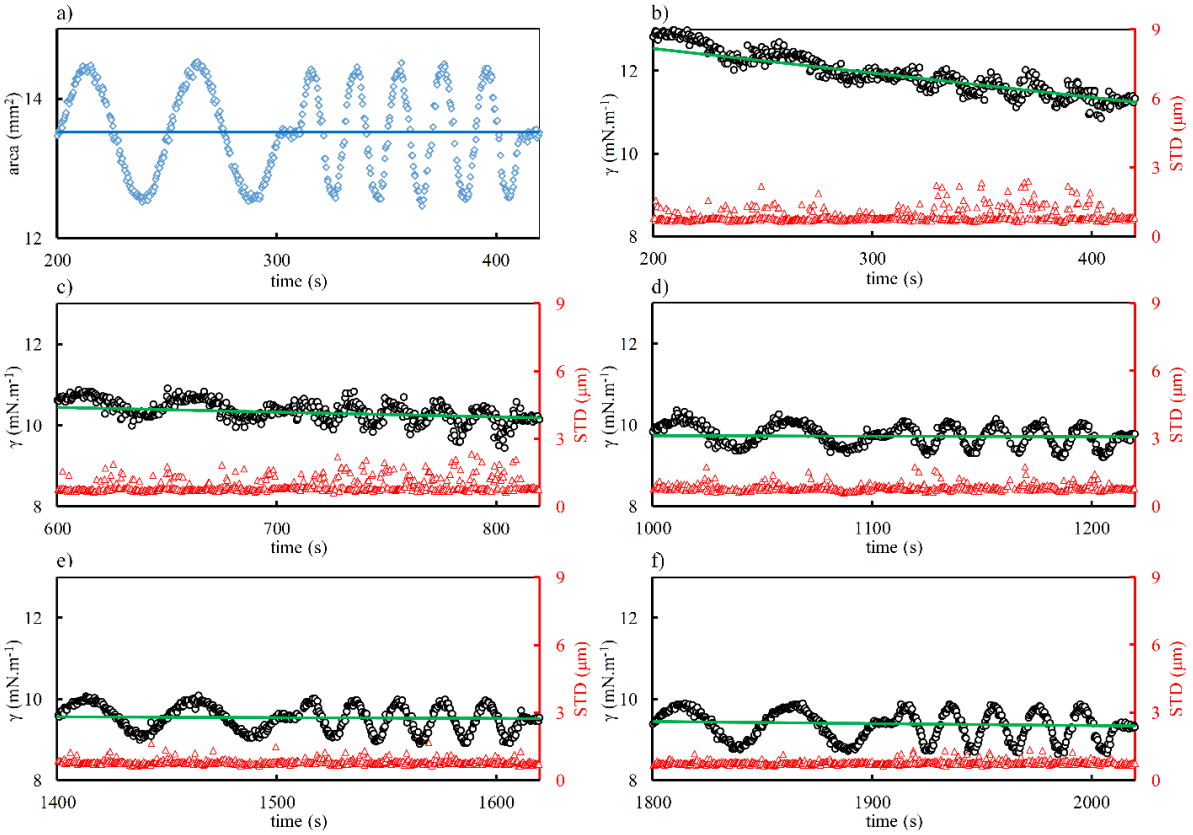

Figure 3- Sinusoidal interfacial area perturbations with a 0.5 mm^3 volumetric amplitude (~1 mm^2 area amplitude) for a 0·3 $mg·mL^{-1}$ lipase aqueous solution droplet with a volume of 5.0 mm^3 formed inside sunflower oil at frequencies of 0.02 and 0.05 Hz versus aging time; ***(a)*** *interfacial area oscillations between 200–420 s (◇) (the curves for the other area oscillations are the same as (a)), the blue line (▬) is the non-oscillating interfacial area of the droplet;* ***(b–f)*** *IFT (○) and STD (△) of the droplet in time intervals between 200–420, 600–820, 1000–1220, 1400–1620, and 1800–2020 s, the green lines (▬) are the non-oscillating IFT trendlines.*

High Concentrations of Lipase

The IFT and STD data recorded during sinusoidal area perturbations for a *2.5 $mg·mL^{-1}$* lipase solution droplet formed in sunflower oil at two frequencies and in different time intervals are shown in Figure 4(a–f). The amplitudes of the IFT responses are increased compared to Figure 3, indicating an increase in the elasticity modulus of the interfacial layer. Several studies have suggested that protein desorption from liquid–fluid interfaces requires high activation energy. The conformational change in the tertiary structure

of adsorbed proteins is the main factor hindering their facile desorption [36].

The IFT response to harmonic area perturbations shows a nonlinear behavior toward later adsorption times, i.e., the half-cycles above and below the non-oscillating IFT trendlines, green lines in the figure, become more asymmetric with time. Area oscillations at two time periods are also shown in Figure 4(g–h) for the sake of comparison. The amplitudes of the half-cycles above the non-oscillating IFT trendlines become larger compared to the ones below the line, indicating that the adsorbed layer is less elastic upon compressing than upon expanding the water–oil interface.

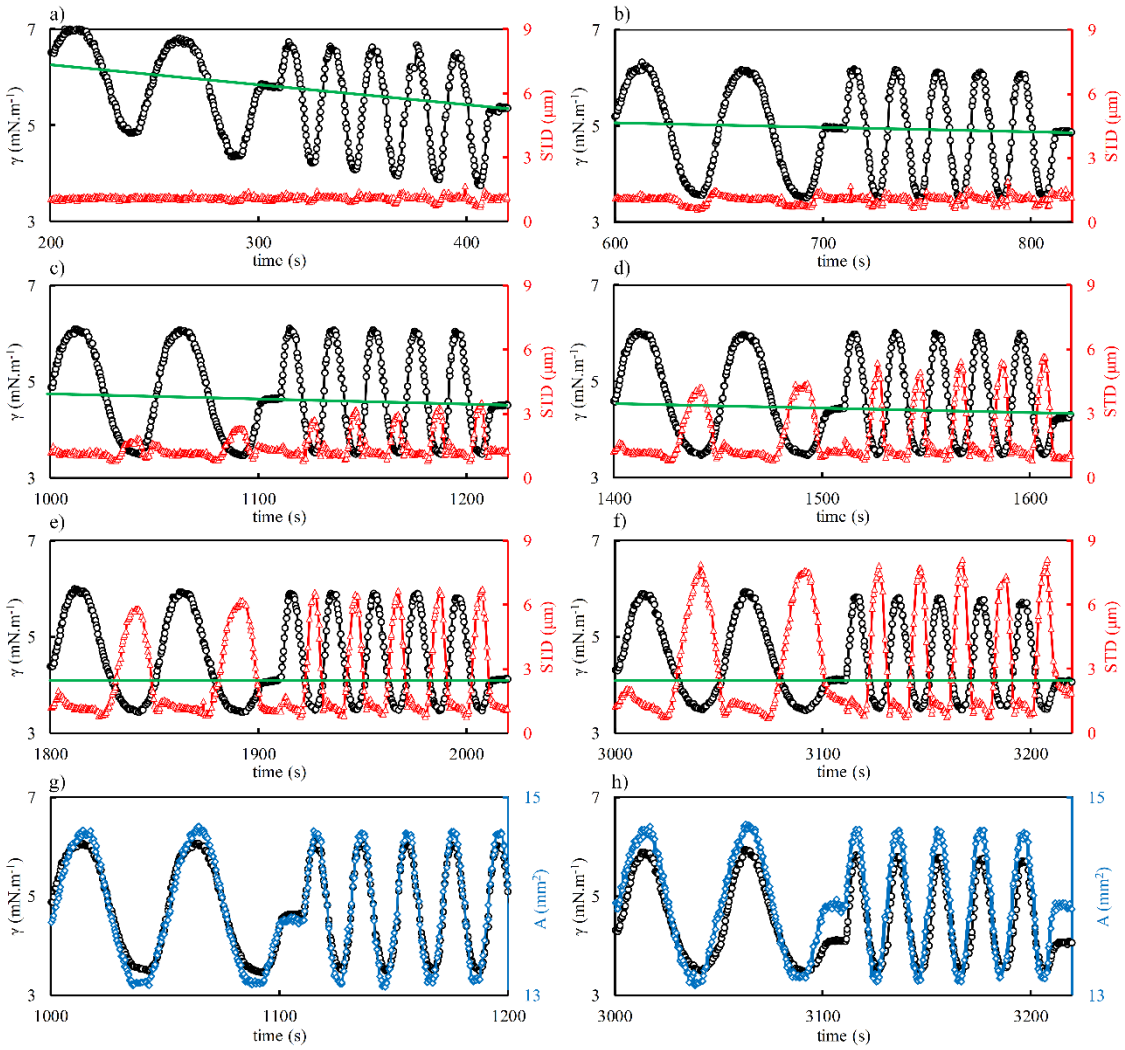

Figure 4- IFT and STD responses to sinusoidal perturbations of the interfacial area with 0.5 mm^3 volumetric amplitude (~1 mm^2 area amplitude) for a 2·5 $mg·mL^{-1}$ lipase aqueous solution droplet with a volume of 5.0 mm^3 inside sunflower oil during 0.02 and 0.05 Hz frequencies versus aging time of the droplet; ***(a–f)*** *interfacial tension (○) and standard deviation (△) of the droplet in time intervals between 200–420, 600–820, 1000–1220, 1400–1620, 1800–2020, 3000–3220 s, green lines (▬) are the non-oscillating IFT trendlines;* ***(g–h)*** *interfacial tension (○) and interfacial area (◇) of the droplet between 1000–1220 and 3000–3220 s (the solid lines are added for better readability of experimental data).*

The STD also behaves differently for the higher lipase concentration shown in Figure 4 compared to the low lipase concentration shown in Figure 3. In the time interval 200–420 s, Figure 4(a), the STD is low and uniform, but it starts undulating after that. Over time, lipases covalently crosslink with each other and non-covalently interact with the low molecular weight reaction products, leading to a skin-like monolayer structure at the interface. The interfacial unfolding of the proteins and intermolecular disulfide bonding are believed to give rise to the formation of this skin-like structure [24, 37] which can be quantified with our novel approach here considering elasticity and STD variations. During compression, this skin wrinkles, affecting the Laplacian shape of the droplet and provoking the increase of the STD values. The formation of folds and wrinkles on the droplet surface marks the breakage of the interfacial monolayer structure [38]. Upon aging and compression, breakages in the monolayer structure of the adsorbed proteins can be detected by an increase in the STD parameter. The maximum deviation from Young–Laplace shape occurs at maximum compression when the strong interaction of the adsorbed lipase and products of the hydrolysis at interface can create skin-like layer which causes drop confinement and deformation with significant wrinkling. During expansion path, the skin-like film is reformed to a rather regular adsorbed layer, and droplet shape can be better fitted by the Young–Laplace equation.

As a result, STD variations is in the opposite direction of the IFT changes during interfacial area oscillations The enzymatic functionality of lipase produces interfacial active components, which can compete with lipase and form a mixed adsorbed layer. Among the products, monoglycerides are more interfacially active than diglycerides and fatty acid salts [22]. Therefore, a possible scenario for observing lower elasticity during the compression path for high lipase concentration is the presence of such small surface-active molecules between lipase macromolecules, covering the available area remaining at the interface. This effect can also be observed from the slight decrease in the equilibrium interfacial tension (Figure 4(b–f)), illustrating a saturated interface with mixed lipase and reaction products. Therefore, such fully occupied mixed adsorbed layer cannot evolve to a lower interfacial tension anymore during the compression path. In addition, small molecules can leave the interface under compression conditions easier than unfolded interlinked lipases. However, a detailed explanation of the other potential mechanisms needs further complementary experiments.

It is noted that, for the compression path of the high concentration cases with high STD values, still the STD values are rather low to have a reasonable fitting between the experimental and numerical drop profile (shown in section 3.5). On the other hand, a range of low values of IFT can be observed earlier before increasing of the STD values. Furthermore, we have also performed IFT measurements via capillary pressure-based measuring method (Oscillating drop and bubble analyzer, known as ODBA setup [39]) for which the IFT results can be also measured reasonably for conditions with drop profile deformation and high STD values and comparable results with PAT could be observed. It is noted however that, for

compression step the STD values are discussed as the main data for indication of transformation of the adsorbed layer to skin-like film in this work.

Nonlinear Dilational Rheology of the Interface between Oil and Aqueous Lipase Solution

The interfacial dilational elasticity is a crucial parameter to show how adsorbed molecules interact with one another. In some cases, whereas the IFT remains constant, the elasticity changes over time, indicating that the interfacial concentration, to a great extent, is unchanged while the adsorbed layer may reconfigure due to molecular-level interactions. The asymmetric IFT responses with respect to the non-oscillating IFT trendlines shown in Figure 4 tell us that elasticities resulting from the half-cycles above or below the lines are not the same since the half-waves do not superimpose and, thus, the compressive and expansive elasticities are different.

The interfacial elasticities of lipase solutions at the water–oil interface over time are shown in Figure 5. For *0.3 mg·mL^{-1}* lipase solution, the IFT response is symmetric, and the conventional elasticity calculations using Eq. 4 were applied. The results show that the elasticities increase with time as the adsorbed amount of lipase increases and the required time for the interfacial unfolding is provided. For the *2.5 mg·mL^{-1}* lipase solution, since the compressive and expansive elasticities are notably different, second-order Fourier polynomials were used to calculate both elasticities. The details of the Fourier analysis of an asymmetric IFT response are provided in the Supporting Information. The elasticities for deformations above the lines increase with time, while the elasticities below these lines decrease. A more densely packed lipase interfacial layer increases the chance of intermolecular forces or even bonding between protein molecules, thereby leading to the formation of a more elastic layer in the half-cycles above the lines. On the other hand, adsorbed lipase molecules hydrolyze triglycerides into fatty acids, diglycerides, monoglycerides, and glycerol. The fatty acids and monoglycerides are interfacial active and compete at the interface with the lipase. The production of these smaller surface-active molecules and their partial displacement from the interface by lipase leads to an elasticity reduction during the interfacial area compression.

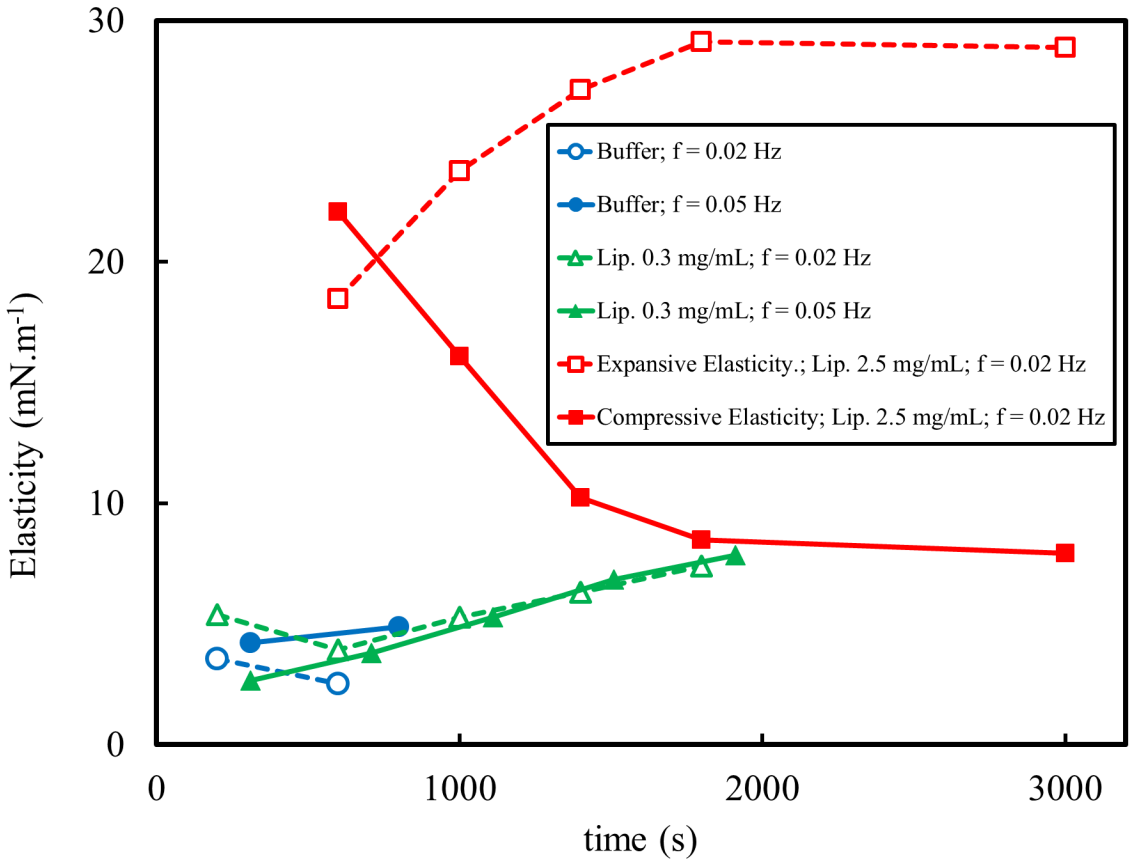

Figure 5- Elasticities for three different aqueous droplets with a volume of 5.0 mm^3 formed in sunflower oil during sinusoidal perturbations of the interfacial area with 0.5 mm^3 volumetric amplitude (~1 mm^2 area amplitude) versus aging time: buffer droplet elasticities during 0.02 (○) and 0.05 (●) Hz frequencies; 0.3 $mg{\cdot}mL^{-1}$ lipase aqueous solution droplet elasticities during 0.02 (△) and 0.05 (▲) Hz frequencies; and 2.5 $mg{\cdot}mL^{-1}$ lipase aqueous solution droplet above (□) and below (■) the equilibrium line during 0.02 Hz frequency (the solid and dashed lines are added for better readability of the experimental data).

Lissajous Plots

When the IFT response deviates from the linear behavior, it can become a function of the path. A viscoelastic interface in the domain of nonlinear IFT response has a memory reflecting its previous states into its present state. The higher this effect is, the higher is the nonlinearity [32]. The Lissajous plot is a way to characterize this hysteresis, demonstrating the evolution of interfacial tension versus interfacial deformation [40, 41]. Due to the interfacial viscosity, the IFT at a specific area deformation is not the same along the periods of expansion and compression, respectively.

When the interfacial layer is not in its equilibrium state, the Lissajous plot shows irregular patterns, i.e., the plot shapes are not repeated at different cycles due to the facile adsorption and desorption given by the weak protein–protein interactions. With ongoing time, the Lissajous plot becomes a closed-loop, or an ellipse under an ideal linear interfacial behavior (Eq. 6), in which the compression path has lower IFT values

than the expansion path in IFT versus A/A_0 plot, i.e., the Lissajous plot. During compression, the interfacial concentration increases, giving rise to lower IFTs. However, some protein molecules should desorb, which is hardly attainable because of the high energy required or the short time available. During expansion, IFT increases owing to the decrease in the interfacial concentration, and adsorption is required to re-achieve the equilibrium state, which is also time- and energy-intensive.

The IFT responses and Lissajous plots of 2.5 $mg \cdot mL^{-1}$ lipase adsorbed layer at the water–air interface are shown in Figure 6 (a). Between 600–700 s, the Lissajous plot has few irregular patterns because the adsorbed layer is not yet completely in equilibrium. In later times, the Lissajous plots are better developed, with the compression path denoted by the purple arrow having smaller IFTs than the expansion path (red arrow), as expected from a nonreactive system.

The IFT responses and Lissajous plots of 2.5 $mg \cdot mL^{-1}$ lipase adsorbed layer at the water–heptane interface are shown in Figure 6 (b) which have smaller amplitudes than at the water–air interface and the deviation from the linear behavior is less pronounced. The hydrophobic lipase chains can penetrate into the organic phase at the water–heptane interface, making the lipase more stable compared to the water–air interface [42, 43]. The Lissajous pattern is repeatable at different consecutive cycles. For the triangular perturbations, Figure 6 (c), the compression period is nearly linear in the Lissajous plot. At different periods, minor changes occur in the IFT response pattern, although the area deformation is generated with a large amplitude.

The Lissajous plots for a 2.5 $mg \cdot mL^{-1}$ lipase solution at the water–SFO interface are shown in Figure 7(a–e). At the beginning of the adsorption process, the patterns are irregular. With increasing time, the IFT during the compression period becomes higher than during the expansion period, in contrast to what we have seen in Figure 6. One explanation can be that, under compression, some adsorbed molecules are displaced from the interface into the proximal sublayer, increasing the IFT to some extent. Also, the proteins compressibility may lead to their compaction and a decrease in the number of protein chains penetrating the interface into the bulk. By releasing the compressive force and letting the interface expand, those molecules and chains return to the adsorbed layer, decreasing the IFT quickly. To draw a solid conclusion, however, the impact of each hydrolysis product on the interfacial rheology should be studied separately.

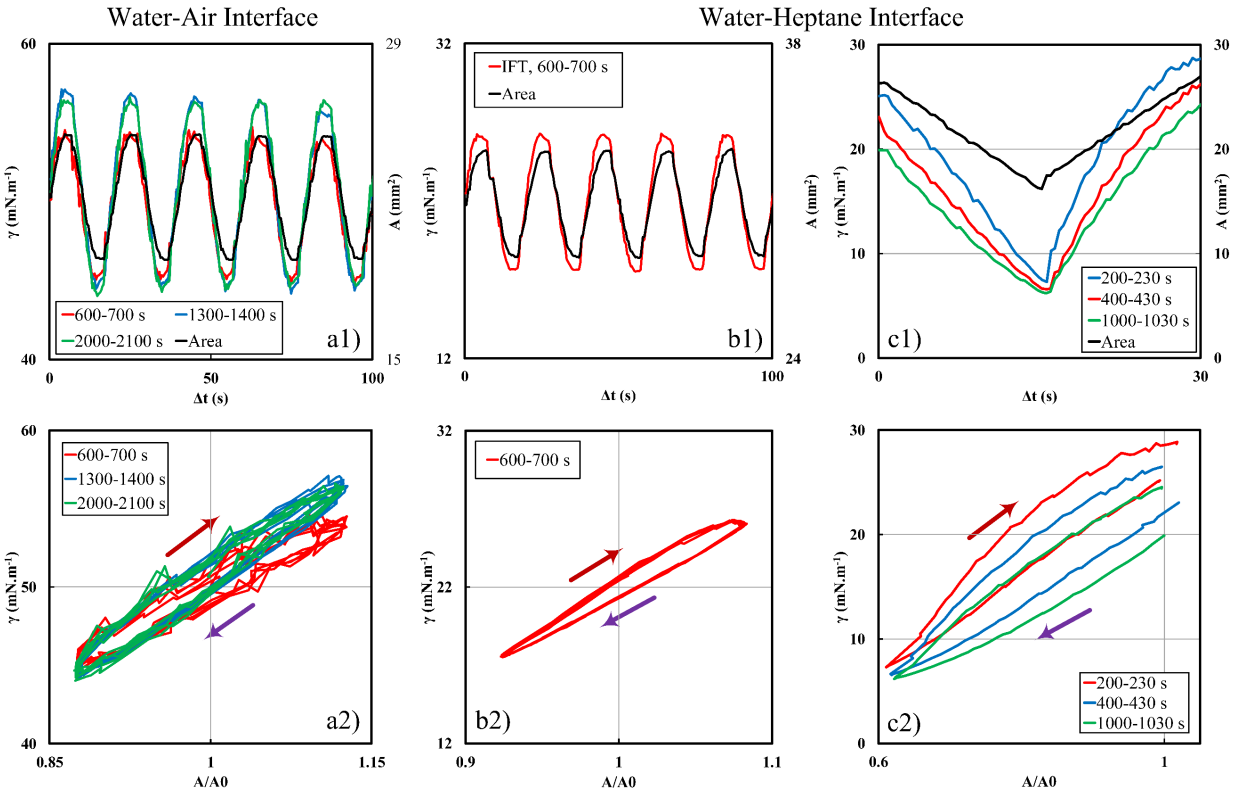

Figure 6 IFT and Lissajous plots of lipase solutions: ***(a)*** *sinusoidal perturbations of water–air interface with 0.05 Hz frequency and 2.7 mm^2 amplitude for 2.5 mg·mL^{-1} lipase solutions (droplet volume of 12.0 mm^3);* ***(b)*** *sinusoidal perturbations of water–heptane interface with 0.05 Hz frequency and 2.7 mm^2 amplitude for 2.5 mg·mL^{-1} lipase solution (droplet volume of 18.0 mm^3);* ***(c)*** *triangular perturbations of water–heptane interface with ~0.03 Hz frequency and 10 mm^2 amplitude for 2.5 mg·mL^{-1} lipase solutions between 200–230, 400–430, and 1000–1030 s (droplet volume of 15.0 mm^3); the purple and red arrows show the direction of compression and expansion, respectively (solid lines are used for better readability of the experimental data).*

At 0.3 mg·mL^{-1} lipase concentration, Figure 7(f), the nonlinearity in the IFT response is not profound, the adsorbed layer is not yet fully developed, and, thus, the Lissajous plots are not conclusive.

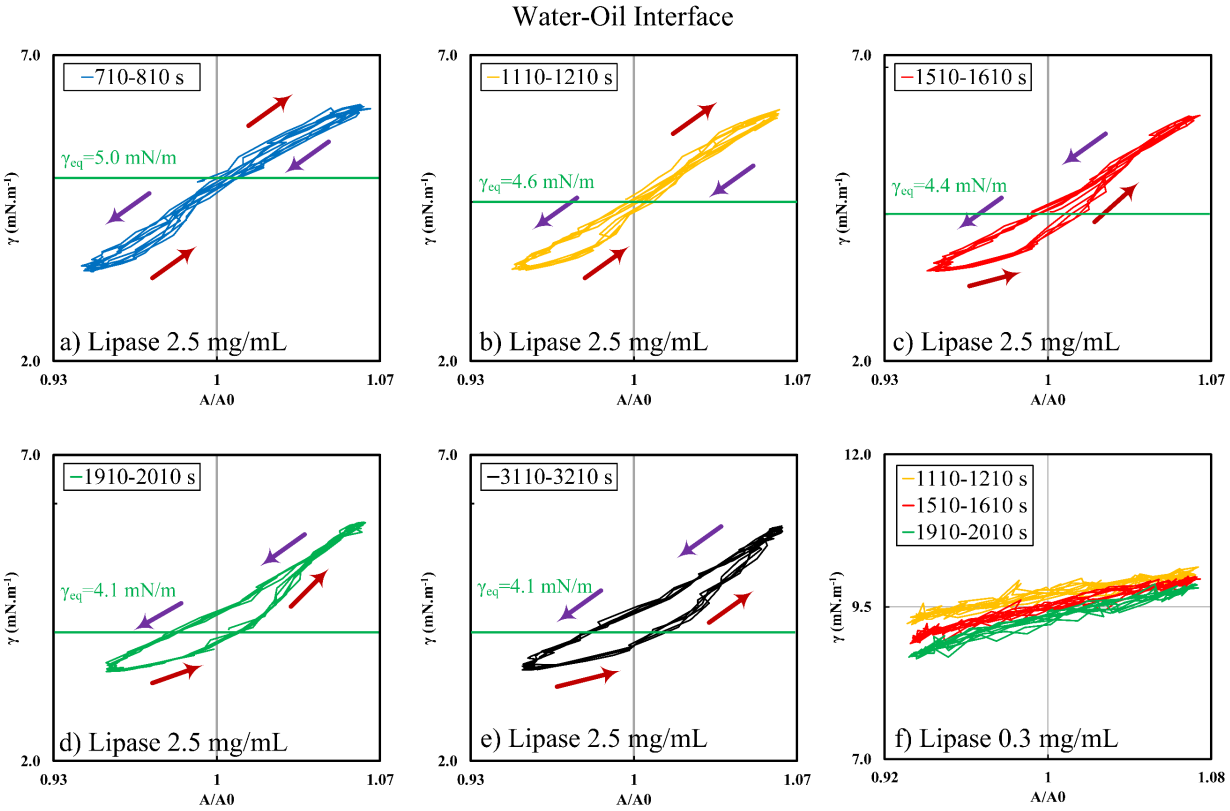

Figure 7 Lissajous plots of the interfacial tension at the water–sunflower oil interface at droplets of 5.0 mm^3 volume: ***(a–e)*** *2.5 mg·mL^{-1} lipase solution during sinusoidal perturbation with 0.5 mm^3 volumetric amplitude (~1 mm^2 area amplitude) and 0.05 Hz frequency between 710–810, 1110–1210, 1510–1610, 1910–2010, and 3110–3210 s;* ***(f)*** *0.3 mg·mL^{-1} lipase solution during sinusoidal perturbation with 0.5 mm^3 volumetric amplitude (~1 mm^2 area amplitude) and 0.05 Hz frequency between 1110–1210, 1510–1610, and 1910–2010 s; the purple and red arrows show the directions of compression and expansion, respectively (solid lines are used for better readability of the experimental data).*

The values of STD versus area deformation for 2.5 mg·mL^{-1} lipase solution is shown in Figure 8(a), illustrating how STD rises along the compression periods. The increase in STD is a sign of the interfacial layer aging, which is why STD increases with time. The sharp increase in the STD marks the breakage point in the monolayer structure of the adsorbed layer. With longer times, the points of STD deflection upon compression occur at higher values of area deformation, meaning that the monolayer structure is broken in larger interfacial areas. This effect indicates that the molar area of the adsorbed protein monolayer increases over time due to interfacial unfolding. Proteins adsorb to an interface in different conformation states, each of which has its molar area. An increase in the interfacial concentration leads to a decrease in the available molar area, while unfolding can increase the required molar area [44, 45]. The STD analysis can be used in parallel with the adsorption isotherm and the interfacial equation of state to further discuss

the protein adsorption states. The droplet shapes of a 2.5 mg·mL^{-1} lipase solution in oil at the maximum and minimum area of a high-amplitude perturbation are also shown in Figure 8(b–c)(1). The wrinkling of the skin-like interfacial structure is well illustrated during the maximum compression of the droplet (Figure 8(c)). The digitized values for the actual profiles and the solutions of the Young–Laplace equation are shown in Figure 8(b–c)(2). The numerical error between the actual and the theoretical profiles increases during the compression, Figure 8(b–c)(3), leading to higher STD values.

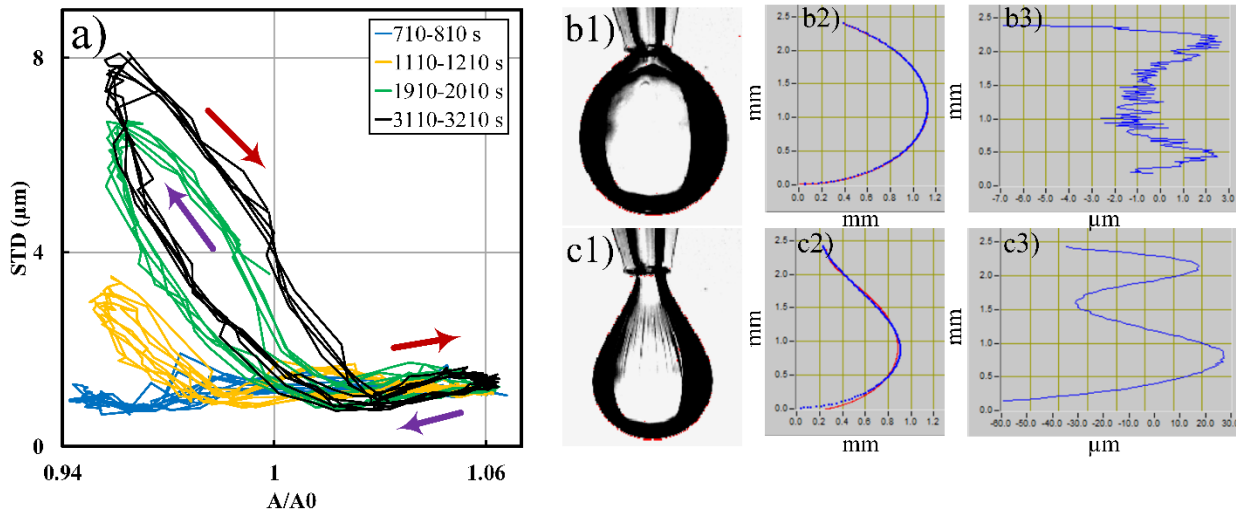

Figure 8 ***(a)*** *Standard deviation of the droplet profile for the water–sunflower oil interface of 2.5 mg·mL^{-1} lipase solution droplets of 5.0 mm^3 volume during sinusoidal perturbation with 0.5 mm^3 volumetric amplitude (~1 mm^2 area amplitude) and 0.05 Hz frequency between 710–810, 1110–1210, 1510–1610, 1910–2010, and 3110–3210 s; the purple and red arrows show the direction of compression and expansion, respectively (solid lines are used for better readability of the experimental data);* ***(b–c)(1)*** *the actual droplet profile for the water–sunflower oil interface of 2.5 mg·mL^{-1} lipase solution with initial droplet volume of 5.0 mm^3 during a sinusoidal perturbation with 1.5 mm^3 volumetric amplitude (~2.5 mm^2 area amplitude, 18% of initial droplet area) and 0.01 Hz frequency at maximum and minimum sizes (1025 and 1075 s);* ***(2)*** *the values of the actual (blue) and the theoretical Young-Laplace droplet profiles (red);* ***(3)*** *the difference between the actual and the theoretical profiles.*

Conclusions

The enzymatic activity of lipase molecules generates new surface-active products, competing with lipase at the water–sunflower oil interface. This enzymatic activity changes the composition of the adsorbed layer. The mixed lipase and hydrolyzed products interactions and adsorption at the water–oil interface can lead to the formation of a skin-like film structure which can influence dynamic interfacial properties significantly. Dynamic surface tensiometry and dilational rheology, as powerful experimental methods, can quantitatively evaluate the evolution of such reactive interfaces.

Analyzing the viscoelastic properties of an enzymatically active water–oil interface suggests how the ongoing reaction leads to interfacial interactions of lipase and products. Here, we discussed how lipase dilational rheology shows a nonlinear IFT-response at the water–sunflower oil interface while the changes

of the dynamic interfacial tension are negligible. In an interfacial layer in the nonlinear domain of IFT responses, the dilational viscoelasticity becomes a function of frequency, amplitude, and path of area deformations. For a lipase aqueous solution drop in oil, the IFT response becomes asymmetric with time: the elasticities during the expansion periods become larger with time, while the elasticities during the compression periods get smaller. Via enzymatic hydrolysis of the sunflower oil, the surface-active products can facilitate desorption upon interface area compression while the adsorbed lipase inhibits adsorption during expansion. Also, the saturation of the interface by products leaves no space for the adsorbed layer to shrink more upon compression, leading to a multilayered configuration upon further compression. These effects result in different responses of the IFT during compressions and expansions.

Over time and upon compression, the standard deviation of the droplet profile compared to the Young–Laplace equation increases significantly. The aging of the lipase adsorbed layer results in a complex formation at the interface. The covalent crosslinking is a reason for the formation of a skin-like adsorbed layer. The interfacial unfolding of the protein molecules and its effect on their molar area in the adsorbed layer can be discussed by the deflection point in the STD versus area deformation plot.

The methodology addressed here can be applied to the interfacial enzymatic reactions to investigate the kinetics of reaction by their effect on the interfacial properties of the system. In future works, a wide range of different factors such as concentration, amplitude, frequency, type of interface, and time should be taken into account to provide more insight into their effect on the IFT-response and viscoelastic properties of the interface. Also, the method should be coupled with other approaches, such as atomic force microscopy, Brewster angle microscopy, spectroscopy, calorimetry, and ellipsometry, to understand the underlying mechanisms in actions better.

Acknowledgment

"Gefördert durch die Deutsche Forschungsgemeinschaft (DFG) - TRR 63 "Integrierte chemische Prozesse in flüssigen Mehrphasensystemen" (Teilprojekt Z1) - 56091768.
Funded by the Deutsche Forschungsgemeinschaft (DFG, German Research Foundation) - TRR 63 "Integrated Chemical Processes in Liquid Multiphase Systems" (subproject Z1) - 56091768.

Supporting Information

The Fourier analysis of asymmetric IFT responses to calculate the compressive and expansive elasticities.

References

1. Svendsen, A., Lipase protein engineering. *Biochim. Biophys. Acta Protein Struct. Mol. Enzymol.* **2000,** *1543* (2), 223-238.

2. The nomenclature of lipids (Recommendations 1976) IUPAC-IUB Commission on Biochemical Nomenclature. *Biochem. J.* **1978,** *171* (1), 21-35.
3. Sankaran, R.; Show, P. L.; Chang, J. S., Biodiesel production using immobilized lipase: feasibility and challenges. *Biofuel Bioprod. Biorefin.* **2016,** *10* (6), 896-916.
4. Freedman, B.; Butterfield, R. O.; Pryde, E. H., Transesterification kinetics of soybean oil 1. *J. Am. Oil Chem. Soc.* **1986,** *63* (10), 1375-1380.
5. Gandhi, N. N., Applications of lipase. *J. Am. Oil Chem. Soc.* **1997,** *74* (6), 621-634.
6. Markley, K. S., *Fatty acids: their chemistry, properties, production, and uses*. Interscience Publishers: 1967.
7. Sridharan, R.; Mathai, I. M., Transesterification reactions. *J. Sci. & Ind. Res.* **1974,** *33(4)* 178-187
8. Freedman, B.; Pryde, E.; Mounts, T., Variables affecting the yields of fatty esters from transesterified vegetable oils. *J. Am. Oil Chem. Soc.* **1984,** *61* (10), 1638-1643.
9. Krawczyk, T., Biodiesel-alternative fuel makes inroads but hurdles remain. *Inform.* **1996,** *7*, 801-815.
10. Ma, F.; Hanna, M. A., Biodiesel production: a review. *Bioresour. Technol.* **1999,** *70* (1), 1-15.
11. Reis, P.; Holmberg, K.; Watzke, H.; Leser, M.; Miller, R., Lipases at interfaces: a review. *Adv. Colloid Interface Sci.* **2009,** *147*, 237-250.
12. Reis, P.; Holmberg, K.; Miller, R.; Krägel, J.; Grigoriev, D. O.; Leser, M. E.; Watzke, H. J., Competition between Lipases and Monoglycerides at Interfaces. *Langmuir* **2008,** *24* (14), 7400-7407.
13. Xu, X.; Skands, A.; Høy, C.-E.; Mu, H.; Balchen, S.; Adler-Nissen, J., Production of specific-structured lipids by enzymatic interesterification: elucidation of acyl migration by response surface design. *J. Am. Oil Chem. Soc.* **1998,** *75* (9), 1179-1186.
14. Sarda, L.; Desnuelle, P., Action de la lipase pancréatique sur les esters en émulsion. *Biochim. Biophys. Acta.* **1958,** *30* (3), 513-521.
15. Verger, R., 'Interfacial activation'of lipases: facts and artifacts. *Trends Biotechnol.* **1997,** *15* (1), 32-38.
16. Jegannathan, K. R.; Abang, S.; Poncelet, D.; Chan, E. S.; Ravindra, P., Production of biodiesel using immobilized lipase—a critical review. *Crit. Rev. Biotechnol.* **2008,** *28* (4), 253-264.
17. Mackie, A. R., Structure of adsorbed layers of mixtures of proteins and surfactants. *Curr. Opin. Colloid Interface Sci.* **2004,** *9* (5), 357-361.
18. Javadi, A.; Dowlati, S.; Miller, R.; Schneck, E.; Eckert, K.; Kraume, M., Dynamics of Competitive Adsorption of Lipase and Ionic Surfactants at the Water–Air Interface. *Langmuir* **2020,** *36* (40), 12010-12022.
19. Verger, R.; Pattus, F.; Pieroni, G.; Riviere, C.; Ferrato, F.; Leonardi, J.; Dargent, B., Regulation by the "interfacial quality" of some biological activities. *Colloids Surf.* **1984,** *10*, 163-180.
20. Aloulou, A.; Rodriguez, J. A.; Fernandez, S.; van Oosterhout, D.; Puccinelli, D.; Carrière, F., Exploring the specific features of interfacial enzymology based on lipase studies. *Biochim. Biophys. Acta Mol. Cell Biol. Lipids* **2006,** *1761* (9), 995-1013.
21. Fave, G.; Coste, T.; Armand, M., Physicochemical properties of lipids: new strategies to manage fatty acid bioavailability. *Cell. Mol. Biol.* **2004,** *50* (7), 815-832.
22. Reis, P.; Miller, R.; Leser, M.; Watzke, H.; Fainerman, V.; Holmberg, K., Adsorption of polar lipids at the water− oil interface. *Langmuir* **2008,** *24* (11), 5781-5786.
23. Reis, P. M.; Raab, T. W.; Chuat, J. Y.; Leser, M. E.; Miller, R.; Watzke, H. J.; Holmberg, K., Influence of surfactants on lipase fat digestion in a model gastro-intestinal system. *Food Biophys.* **2008,** *3* (4), 370.
24. Reis, P.; Miller, R.; Kragel, J.; Leser, M.; Fainerman, V.; Watzke, H.; Holmberg, K., Lipases at interfaces: unique interfacial properties as globular proteins. *Langmuir* **2008,** *24* (13), 6812-6819.
25. del Castillo-Santaella, T.; Maldonado-Valderrama, J.; Cabrerizo-Vílchez, M. Á.; Rivadeneira-Ruiz, C.; Rondón-Rodriguez, D.; Gálvez-Ruiz, M. a. J., Natural Inhibitors of Lipase: Examining Lipolysis in a Single Droplet. *Journal of Agricultural and Food Chemistry* **2015,** *63* (47), 10333-10340.
26. Dowlati, S.; Javadi, A.; Miller, R.; Bahramian, A., Characterization of reactive interfaces via coupled interfacial tension measurements and interphase mass transfer analysis. *Colloids and Surfaces A:*

Physicochemical and Engineering Aspects **2021,** *609*, 125711.
27. Gaonkar, A. G., Interfacial tensions of vegetable oil/water systems: Effect of oil purification. *J. Am. Oil Chem. Soc.* **1989,** *66* (8), 1090-1092.
28. Loglio, G.; Pandolfini, P.; Miller, R.; Makievski, A. V.; Krägel, J.; Ravera, F.; Noskov, B. A., Perturbation–response relationship in liquid interfacial systems: non-linearity assessment by frequency–domain analysis. *Colloids Surf. A Physicochem. Eng. Asp.* **2005,** *261* (1-3), 57-63.
29. Zholob, S.; Fainerman, V.; Kovalchuk, V.; Makievski, A.; Krägel, J.; Miller, R., Determination of the dilational elasticity and viscosity from the surface tension response to harmonic area perturbations. In *Interfacial rheology*, Brill Publ.: 2009; pp 38-76.
30. Loglio, G.; Tesei, U.; Cini, R., Dilational properties of monolayers at the oil-air interface. *J. Colloid Interface Sci.* **1984,** *100* (2), 393-396.
31. Loglio, G.; Tesei, U.; Cini, R., Viscoelastic dilatation processes of fluid/fluid interfaces: time-domain representation. *Colloid Polym. Sci.* **1986,** *264* (8), 712-718.
32. Bykov, A.; Liggieri, L.; Noskov, B.; Pandolfini, P.; Ravera, F.; Loglio, G., Surface dilational rheological properties in the nonlinear domain. *Adv. Colloid Interface Sci.* **2015,** *222*, 110-118.
33. Christopher, L. P.; Kumar, H.; Zambare, V. P., Enzymatic biodiesel: challenges and opportunities. *Appl. Energy* **2014,** *119*, 497-520.
34. Dopierala, K.; Javadi, A.; Krägel, J.; Schano, K.-H.; Kalogianni, E.; Leser, M.; Miller, R., Dynamic interfacial tensions of dietary oils. *Colloids Surf. A Physicochem. Eng. Asp.* **2011,** *382* (1-3), 261-265.
35. Zholob, S.; Kovalchuk, V.; Makievski, A.; Krägel, J.; Fainerman, V.; Miller, R., Determination of the dilational elasticity and viscosity from the surface tension response to harmonic area perturbations. In *Interfacial rheology*, Brill Publ.: 2009; pp 77-102.
36. Shimizu, M.; Ametani, A.; Kaminogawa, S.; Yamauchi, K., The topography of αs1-casein adsorbed to an oil/water interface: an analytical approach using proteolysis. *Biochim. Biophys. Acta Protein Struct. Mol. Enzymol.* **1986,** *869* (3), 259-264.
37. Lu, G.; Chen, H.; Li, J., Forming process of folded drop surface covered by human serum albumin, β-lactoglobulin and β-casein, respectively, at the chloroform/water interface. *Colloids Surf. A Physicochem. Eng. Asp.* **2003,** *215* (1-3), 25-32.
38. Vatanparast, H.; Javadi, A.; Bahramian, A., Silica nanoparticles cationic surfactants interaction in water-oil system. *Colloids Surf. A Physicochem. Eng. Asp.* **2017,** *521*, 221-230.
39. Javadi, A.; Krägel, J.; Makievski, A. V.; Kovalchuk, V. I.; Kovalchuk, N. M.; Mucic, N.; Loglio, G.; Pandolfini, P.; Karbaschi, M.; Miller, R., Fast dynamic interfacial tension measurements and dilational rheology of interfacial layers by using the capillary pressure technique. *Colloids and Surfaces A: Physicochemical and Engineering Aspects* **2012,** *407*, 159-168.
40. Sagis, L. M. C., Dynamic properties of interfaces in soft matter: Experiments and theory. *Rev. Mod. Phys.* **2011,** *83* (4), 1367-1403.
41. Sagis, L. M. C.; Fischer, P., Nonlinear rheology of complex fluid–fluid interfaces. *Curr. Opin. Colloid Interface Sci.* **2014,** *19* (6), 520-529.
42. Pradines, V.; Krägel, J. r.; Fainerman, V. B.; Miller, R., Interfacial properties of mixed β-lactoglobulin− SDS layers at the water/air and water/oil interface. *J. Phys. Chem. B* **2009,** *113* (3), 745-751.
43. Dan, A.; Kotsmar, C.; Ferri, J. K.; Javadi, A.; Karbaschi, M.; Krägel, J.; Wüstneck, R.; Miller, R., Mixed protein–surfactant adsorption layers formed in a sequential and simultaneous way at water–air and water–oil interfaces. *Soft Matter* **2012,** *8* (22), 6057-6065.
44. Fainerman, V.; Miller, R.; Wüstneck, R., Adsorption of proteins at liquid/fluid interfaces. *J. Colloid Interface Sci.* **1996,** *183* (1), 26-34.
45. Fainerman, V.; Lucassen-Reynders, E.; Miller, R., Description of the adsorption behaviour of proteins at water/fluid interfaces in the framework of a two-dimensional solution model. *Adv. Colloid Interface Sci.* **2003,** *106* (1-3), 237-259.

TOC

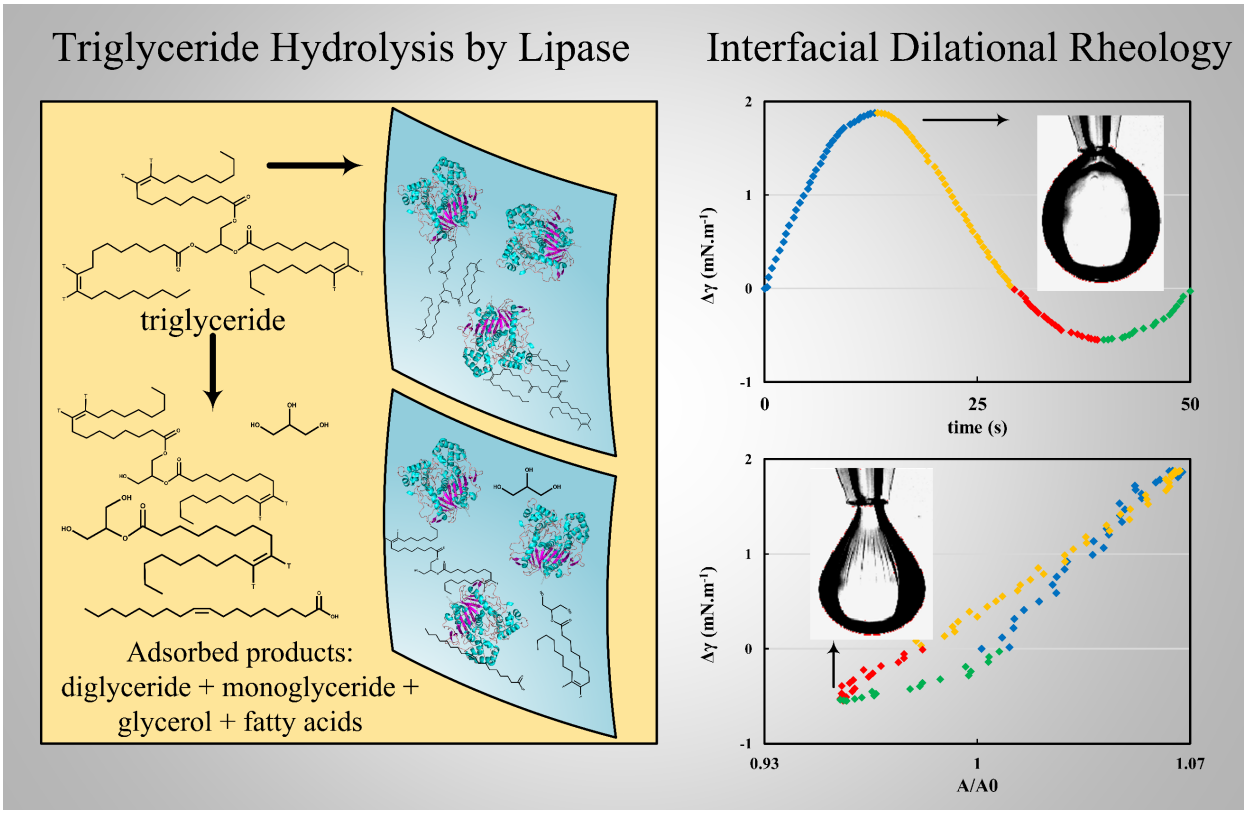
Triglyceride Hydrolysis by Lipase
triglyceride
Adsorbed products:
diglyceride + monoglyceride +
glycerol + fatty acids
Interfacial Dilational Rheology
Δγ (mN.m-1)
time (s)
Δγ (mN.m-1)
A/A0